Chemosphere 275 (2021) 130066

Contents lists available at ScienceDirect

Chemosphere

journal homepage: www.elsevier.com/locate/chemosphere

Optimization of a low flow sampler for improved assessment of gas and particle bound exposure to chlorinated paraffins

Insam Al Saify [a, b], Lara Cioni [a], Louise M. van Mourik [b], Sicco H. Brandsma [b], Nicholas A. Warner [a, c, *]

[a] NILU-Norwegian Institute for Air Research, Fram Centre, NO-9296, Tromsø, Norway
[b] Vrije Universiteit, Department of Environment and Health, Faculty of Sciences, De Boelelaan 1085, 1081 HV, Amsterdam, the Netherlands
[c] UiT-The Arctic University of Norway, Department of Arctic and Marine Biology, Hansine Hansens Veg 18, 9037, Tromsø, Norway

HIGHLIGHTS

- Improved methodology for assessment of airborne exposure to chlorinated paraffins.
- Lower detection limits and sampling variation with optimized sampler design.
- No saturation for gas and filter phases after 7 days of continuous sampling.
- Separation of gas and particle phases avoids over/underestimation in quantification.
- Presence of vSCCPs in indoor air represent an emerging human inhalation risk.

GRAPHICAL ABSTRACT

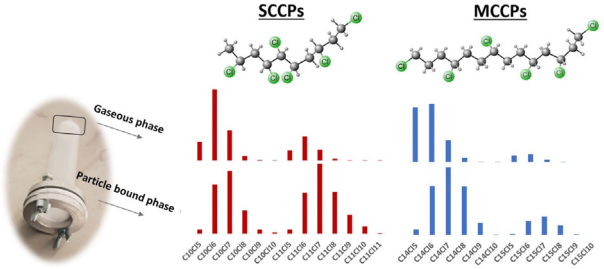

ARTICLE INFO

Article history:
Received 5 January 2021
Received in revised form
15 February 2021
Accepted 20 February 2021
Available online 23 February 2021

Handling Editor: R Ebinghaus

Keywords:
Chlorinated paraffins
Air sampler
Air monitoring
Indoor air
Particulate matter
Method development

ABSTRACT

An optimized low volume sampler was developed to determine both gas- and particle bound concentrations of short and medium-chain chlorinated paraffins (S/MCCPs). Background contamination was limited by the sampler design, providing method quantification limits (MQLs) at least two orders of magnitude lower than other studies within the gas (MQL: 500 pg (ΣSCCPs), 1.86 ng (ΣMCCPs)) and particle (MQL: 500 pg (ΣSCCPs), 1.72 ng (ΣMCCPs) phases. Good repeatability was observed between parallel indoor measurements (RSD $\leq$ 9.3% (gas), RSD $\leq$ 14% (particle)) with no breakthrough/saturation observed after a week of continuous sampling. For indoor air sampling, SCCPs were dominant within the gas phase (17 $\pm$ 4.9 ng/m^3) compared to MCCPs (2.7 $\pm$ 0.8 ng/m^3) while the opposite was observed in the particle bound fraction (0.28 $\pm$ 0.11 ng/m^3 (ΣSCCPs) vs. 2.7 $\pm$ 1.0 ng/m^3 (ΣMCCPs)). Only SCCPs in the gas phase could be detected reliably during outdoor sampling and were considerably lower compared to indoor concentrations (0.27 $\pm$ 0.10 ng/m^3). Separation of the gas and particle bound phase was found to be crucial in applying the appropriate response factors for quantification based on the deconvoluted S/MCCP sample profile, thus avoiding over- (gas phase) or underestimation (particle phase) of reported concentrations. Very short chain chlorinated paraffins (vSCCPs, C_5-C_9) were also detected at equal or

* Corresponding author. Department of Environmental Chemistry, NILU-Norwegian Institute for Air Research, Fram Centre, Hjalmar Johansens gate 14, NO-9296, Tromsø, Norway.
E-mail addresses: nicholas.warner@nilu.no, nw@nilu.no (N.A. Warner).

https://doi.org/10.1016/j.chemosphere.2021.130066

higher abundance compared to SCCP congener groups (C_{10}-C_{13}) congener groups, indicating an additional human indoor inhalation risk.

1. Introduction

Chlorinated paraffins (CPs) have emerged as a significant research area due to the growing recognition of the (potential) hazards they pose to both human and environmental health (Chen et al., 2019). Produced by radical chlorination of *n*-alkanes from petroleum distillation, they consist of complex mixtures of polychlorinated *n*-alkanes (>100,000s congeners) of varying carbon chain length and degree of chlorination. Hence, the physical-chemical properties vary widely among the different congeners making them desirable for many applications (e.g., additives, paints, coatings, plasticizers and flame retardants). They can be classified according to their carbon chain length in short- (C_{10}-C_{13}), medium- (C_{14}-C_{17}) or long- ($C_{\geq 18}$) chain or degree of chlorination (30–70%) (van Mourik et al., 2015).

Their high production (global production of >1 million tonnes/year) (Glüge et al., 2016) and presence in remote sites have driven the need for greater awareness and investigation towards their fate in the environment. Short-chain chlorinated paraffins (SCCPs) were nominated for persistent organic pollutant (POP) candidacy in 2006 but have only recently been added to Annex A (elimination) of the Stockholm Convention on POPs (UNEP, 2017). Meanwhile, medium- and long-chain CPs (MCCPs and LCCPs) are still under evaluation due to knowledge gaps about their environmental transport and fate (Glüge et al., 2018). Delay in regulation of CPs is attributed to the analytical challenges of accurately measuring these substances to provide data for regulators to evaluate (Chen et al., 2019; Schinkel et al., 2018).

Levels of SCCPs are expected to decline with adoption of recent regulations, although exposure will continue to occur through emission from materials still in use. In addition, greater exposure of MCCPs and LCCPs is expected as they replace SCCPs as alternative chemicals (Dick et al., 2010; Zeng et al., 2017). Based on their physical chemical properties, SCCPs and MCCPs can be emitted to air and remain in the gas and/or particle phase, posing a human inhalation risk, particularly within indoor environments (Fridén et al., 2011). However, trace analysis is difficult due to high background contamination and variation resulting in elevated detection limits and hampering results. Previous studies have investigated SCCPs and MCCPs within indoor air using active sampling techniques but have combined gas and particle phase extracts to report total airborne exposure (Fridén et al., 2011; Sakhi et al., 2019) or collected particulate matter only (Zhou et al., 2018), losing information on the congener group profile distribution across the gas and particle phases. For assessment of outdoor atmospheric concentrations of CPs, high volume samplers are often used to obtain sufficient mass of analyte to overcome background contamination. However, polyurethane foam (PUF) is often used as a sampling media which can introduce a significant co-extracted matrix into samples, potentially hindering analytical performance. PUF may also possibly contribute to higher background levels of CPs and thus larger volumes need to be collected (>200 m^3) to obtain concentrations over detection limits (Wang et al., 2012, 2019).

In this study, we describe the optimization of a simple but innovative low volume sampler design capable of conducting simultaneous measurements of CPs within the gas and particle phase fractions. The developed sampler performance was assessed for both indoor and outdoor environments monitoring S/MCCPs to study congener group profiles between gas and particle phase exposure and improve upon data accuracy in reporting airborne concentrations.

2. Methods and materials

2.1. Preparation of active air sampler

The active air sampler was developed and modified based on a previous design published by Warner et al. (2020). Collection of air samples were carried out in parallel using 25 mL SPE cartridges packed with ABN Express sorbent (120 mg, 50 μm particle diameter, Biotage, Sweden) equipped with a filter template, constructed by Innovation Norwegian Institute for Air Research (NILU) AS, to collect both the gas and particle phase fractions for CP analysis (Fig. 1). A glass microfiber filter (Whatman Grade GF/C, 90 mm diameter, 1.2 μm particle retention) was installed into the filter template to collect and separate the particle fraction.

The filter template consists of three stainless-steel metal support rings, a metal mesh filter to support the glass microfiber filter and a metal top plate equipped with a Teflon-O-ring to ensure an airtight seal during transport. The surface area of the filter exposed to air is ±8.55 cm^2.

Sampler preparation and extraction work was performed in an ISO class 6 clean room facility equipped with both gas- and particle filtration to avoid or minimize background contamination. All glassware (as well as the glass microfiber filters) were heated to 450 °C overnight, rinsed with *n*-hexane and left to dryness. All stainless-steel components of the filter template were sonicated in DCM/*n*-hexane (1:1) for 10 min and allowed to dry before use.

The SPE sorbent cartridges were packed and prepared using the same protocol described by Warner et al. (2020). The glass microfiber filters were cleaned using a Büchner funnel filtration set-up connected to a vacuum pump. The Büchner funnel was pre-rinsed with *n*-hexane before the filter was placed on the plate. The filters were washed using 15 mL of DCM followed by 15 mL of *n*-hexane. The solvents were allowed to drain through the filter under ambient pressure. Subsequently, vacuum was applied to the filter flask for 2 min to dry the filters. The air samplers were pre-assembled inside the clean room facility and sealed with the stainless-steel top plate fitted with a Teflon O-ring and luer tip to ensure an airtight seal and prevent contamination during transport. Further details about the materials are provided in the Supporting Information (SI).

2.2. Sample deployment and collection

Indoor- and outdoor sampling was performed in parallel to evaluate repeatability and quality assurance of the active air sampler (AAS) for both gas and particle bound fractions. Samples of the gas- and particulate phase were collected both inside the atrium of the Fram Centre (Tromsø, Norway (69°38′37.3″N 18°56′54.3″E)) and outside approximately 50 m away from Fram Centre using the same sampling design described by Warner et al. (2020) (Fig. S1). Parallel samplers were mounted at a consistent height (~1.2 m above ground), allowing air to circulate freely around them. Two parallel samplers were installed in a downwards

Fig. 1. Active air sampler used to collect both the gas and particle phase of the CPs. Left the modified sampler and right the schematic overview of the sampler template.

facing direction with plastic rain shields used to protect the samplers from precipitation and wind to avoid precipitation from entering the template during outdoor sampling (schematic set-up shown in Fig. S1). Indoor sampling design was carried out in a manner similar to outdoor set-up to remain consistent for data comparison. For every sample, one field blank was collected by deploying a clean SPE cartridge and glass microfiber filter installed the same sampling height for 30 s without turning on the pump. After sample collection, the top plate containing the Teflon O-ring and PE luer tip were reinstalled at the inlet and outlet ends of the sampler, respectively, and transported to the clean room. The glass microfiber filters were removed from the filter template and stored in a clean 15 mL glass test-tube and closed with a PTFE lined cap while the SPE cartridge inlets were sealed with a clean PE cork. Both SPE cartridges and glass microfiber filters were stored at −20 °C until extraction.

Air sampling was collected over time ranges varying from 18h to 168h to determine its performance regarding sampling breakthrough, repeatability, and saturation point (details described in SI). The sampling rate for the AAS was 1.02 ± 0.06 m^3 $hour^{-1}$ (24.5 ± 1.4 m^3 day^{-1}).

2.3. Extraction and clean-up

Before extraction of the sorbent cartridges, all samples were spiked to the upper frit with 50 μL of the CP internal standard ^{13}C-hexachlorodecane (92 pg/μL). The sorbent was eluted slowly using an optimized volume (Cioni et al., 2018) of 5 mL of hexane and collected into a glass test-tube. The extract was reduced to 1 mL using a miVac centrifugal vacuum concentrator (SP Scientific, PA, USA) and purified through a column with 0.7 g of acidified silica (33% w/w) and 0.3 g anhydrous Na_2SO_4 (heated at 600 °C for 8h). The column was precleaned with 15 mL DCM and 15 mL *n*-hexane. After loading the extract, the sample was eluted with 10 mL of 15% DCM/*n*-hexane. The eluent was concentrated to approximately 150 μL and quantitatively transferred with isooctane into a crimped cap GC vial with micro insert. The extract was concentrated further to approximately 50 μL isooctane under a gentle nitrogen stream and 20 μL of the TCN (1, 2, 3, 4 − tetrachloronapthalene) was added as a syringe standard (7.2 pg/μL) prior to analysis. The vials were stored at −20 °C until instrumental analysis. The glass microfiber filters were extracted in the same test tube in which they were stored. Prior to extraction, the sample was spiked with 50 μL of the CP internal standard ^{13}C-hexachlorodecane (92 pg/μL) followed by 10 mL of 1:1 DCM/*n*-hexane. The tubes were sonicated for 15 min followed by shaking on the orbital shaker for 1 h. The extracts were centrifuged for 10 min and the supernatants were transferred into new clean test tubes. The extracts were concentrated to 1 mL and cleaned up using the same procedure as described for the sorbent cartridges.

The recoveries of the ^{13}C-hexachlorodecane ranged from 51 to 56% and were consistent over all experiments, thus independent of the sampling duration. All samples (sorbent and filter) were corrected with their obtained recovery factor. Due to the lack of commercially available labelled standards for MCCPs, concentrations of MCCPs detected on both the sorbent and filter were corrected by the same factor to be compared to SCCP concentrations for discussion purposes.

2.4. Instrumental analysis and quantification

The analysis was performed on a Q Exactive GC Orbitrap MS coupled with a TRACE 1310 GC and was equipped with a TriPlus RSH autosampler (ThermoFisher Scientific, Waltham, MA, USA) and a programmable temperature vaporization (PTV) injector (Agilent

Technologies, Santa Clara, CA, US). Samples were analyzed on a Thermo Scientific TG-5SILMS (15 m × 0.25 mm x 0.25 μm) with an integrated safeguard (10 m) column with helium as carrier gas. The MS was operated in ECNI (70 eV) with methane as reagent gas having a flow rate of 1.4 mL/min. The analysis was performed in full scan over the *m/z* range of 250–750 at a mass resolution of 60,000. Sample injection volume of 1 μL at 90 °C using programable temperature vaporization (PTV) using a temperature program previously published procedure by Krätschmer et al. (2019). Extracted analyte response was determined using TraceFinder 4.1 (ThermoFisher Scientific) with a mass accuracy of 5 ppm.

Quantification was performed based on the procedure reported by Bogdal et al. (2015), where all samples showed goodness of fit values of R^2 = 0.75–0.99. All samples were blank corrected and their concentrations were calculated using the same sample contribution derived from the Lawson and Hanson algorithm (Bogdal et al., 2015). Six commercially available technical formulations (SCCP 51.5%, 55%, 63% Cl and MCCP 42%, 52%, 57% Cl) (Dr. Ehrenstorfer GmbH's laboratory; Augsburg, Germany) and two additional single-chain length standards (C_{10} and C_{11}, 50.18% and 50.21% Cl, respectively) (LGC Standards; Wesel, Germany) were used to construct four-point calibration curves ranging from 0.5 ng/uL to 5 ng/uL with linear response observed (R^2 > 0.99) for both SCCPs and MCCPs (Fig. S2).

A total of 28 SCCP congener groups (expressed as C_mCl_n, $C_{10\text{-}13}Cl_{5\text{-}12}$), 22 MCCP ($C_{14\text{-}17}Cl_{5\text{-}10}$) and vSCCP ($C_{5\text{-}9}Cl_{5\text{-}10}$) congener groups were monitored. The most abundant signal of the $[M\text{-}Cl]^-$ or $[M\text{-}HCl]^-$ isotope cluster were extracted from the full-scan spectra. The isotope cluster selected for evaluation was congener group dependent; the lower chlorinated paraffins tend to lose HCl rather than Cl resulting in greater abundances for the $[M\text{-}HCl]^-$ cluster. The exact *m/z* values of the most abundant ion for each congener group are listed in Table S1-2 and were used consistently between the reference standards and samples.

3. Results and discussion

3.1. Sampler performance

3.1.1. Detection limits

Field blanks (n = 16) observed for the ΣSCCPs were mainly attributed to random electrical signal with concentrations <0.01% compared to the lowest sample concentration measured (100 pg/m^3) in both gas and particle phase and therefore considered negligible. Based on the integrated chemical/instrumental noise observed in the blanks, a threshold of 500 pg (30 pg/m^3) was set based on a signal/noise ratio equal to 10 of our lowest sampled volume (18 m^3) to avoid any contribution from the background signal. The field blank (n = 14) concentrations of the ΣMCCPs were ≤3% of the detected samples for the gaseous and particle bound MCCPs, respectively. As blank contribution was removed from the sample, the method detection limit (MDL) and quantification (MQL) limit for the ΣMCCPs were calculated as three and ten times, respectively, the standard deviation observed in the blanks, shown in Table S4. The MQL were 1.86 and 1.72 ng (0.011–0.103 and 0.010–0.096 ng/m^3 when volumes of 18–169 m^3 were collected) for the gaseous and particle bound MCCPs, respectively. For analytical performance comparison, we have also calculated our detection/quantification limits for MCCPs in a similar manner defined in previous studies (average blank response plus three times the standard deviation) investigating CPs within air. The MQLs were 2.10 and 1.92 ng (0.012–0.116 and 0.011–0.107 ng/m^3 when volumes of 18–169 m^3 were collected) for the gaseous and particle bound MCCPs, respectively. Detection/quantification limits reported here are at least two orders of magnitude lower compared to previous studies using low volume samplers (Table S5). Blank values reported by Ma et al. (2014) using high volume sampling (i.e., 2.6 ng/PUF, 1.2 ng/GFF for S/MCCPs) were comparable to MQLs presented in this study for MCCPs. However, it should be noted that comparison of concentrations and detection limits using different quantification strategies should be done with caution (van Mourik et al., 2018). Lower MDL/MQL levels reported in our study can be attributed to sampler design and the use of a clean room facility for the sample preparation and extraction to avoid exposure sources within indoor environments. This highlights the importance that suitable precautions for both controlling and monitoring background contamination are necessary to ensure data accuracy.

3.1.2. Sampling Repeatability

The percent relative standard deviation (%RSD) for replicate samples in indoor- and outdoor environments were assessed to evaluate the AAS. The indoor CP concentration adsorbed to the sorbent provides good repeatability with RSD ranging from 0.5 to 5.3% for the ΣSCCPs and 4.1–9.3% for the MCCPs at sampling experiments of 18–72h (Fig. 2). Due to sample loss during the extraction procedure, the %RSD of the 69h filter experiment could not be assessed. However, the remaining measurements of the particle bound CPs are in acceptable agreement (≤15%) with RSD ranging from 2.2 to 6.1% for the ΣSCCPs and from 3.4 to 14% for the ΣMCCPs.

Comparable RSDs (2.2–10%) were observed for the ΣSCCPs on the sorbent during outdoor experiments. The gaseous ΣMCCPs and the particle bound ΣSCCPs were both below detection limits and therefore not used for the evaluation. The RSDs of the ΣMCCPs on the filter were higher than those observed during indoor measurements (RSDs >30%). This is likely due to environmental conditions (i.e., precipitation, wind) potentially affecting particle distribution between parallel samplers. As the sorbent is protected by the filter template, it will be less affected by those factors, which may explain the lower %RSD on the sorbent between replicate samplers.

3.1.3. Breakthrough and Saturation assessment

Sorbent breakthrough was assessed indoors by connecting two SPE cartridges in tandem with continuous sampling over a 5-day period. The ΣSCCP and ΣMCCP concentrations on the back SPE cartridge (0.04 ng/m^3 and <MDL, respectively) were negligible compared to the concentrations observed on the front SPE cartridge (12 ng/m^3 and 1.3 ng/m^3). Breakthrough assessment of the individual chain lengths can be found in Table S6. Breakthrough of the ΣSCCPs and ΣMCCPs was 0.32%, and 1.1%, respectively, indicating that breakthrough of SCCPs and MCCPs within the gas phase was minimal. We performed saturation assessment to support the breakthrough experiment by determining the analyte mass behavior on the sorbent and filter over time. As acceptable RSDs (<15%) for gas and particle phases were obtained for SCCPs and MCCPs, one sample was collected for every time point. Fig. 3A shows the ΣSCCPs and ΣMCCPs profiles observed on the sorbent after 7 days (168 h) of sampling. The mass of both ΣSCCPs and ΣMCCPs follow a linear (R^2 of 0.99 and 0.98, respectively) trend over the 7-day sampling period. The air collection of day 5 (119 h) and 7 (168 h) were affected by high MCCP blank levels (sorbent and filter masses of 48 and 75 ng and 23 and 14 ng, respectively: Table S4). The MCCP blanks were averaged and corrected for the two collection points as they were extracted on the same day. Their levels were, however, not included in the quality assurance and control after being determined as outliers (Grubb's test; $\alpha = 0.05$; n = 16, Fig. S3). For all detectable S/MCCP congener groups, a linear relationship was observed during the sampling period of 7 days (168 h), indicating that no saturation on the sorbent occurred

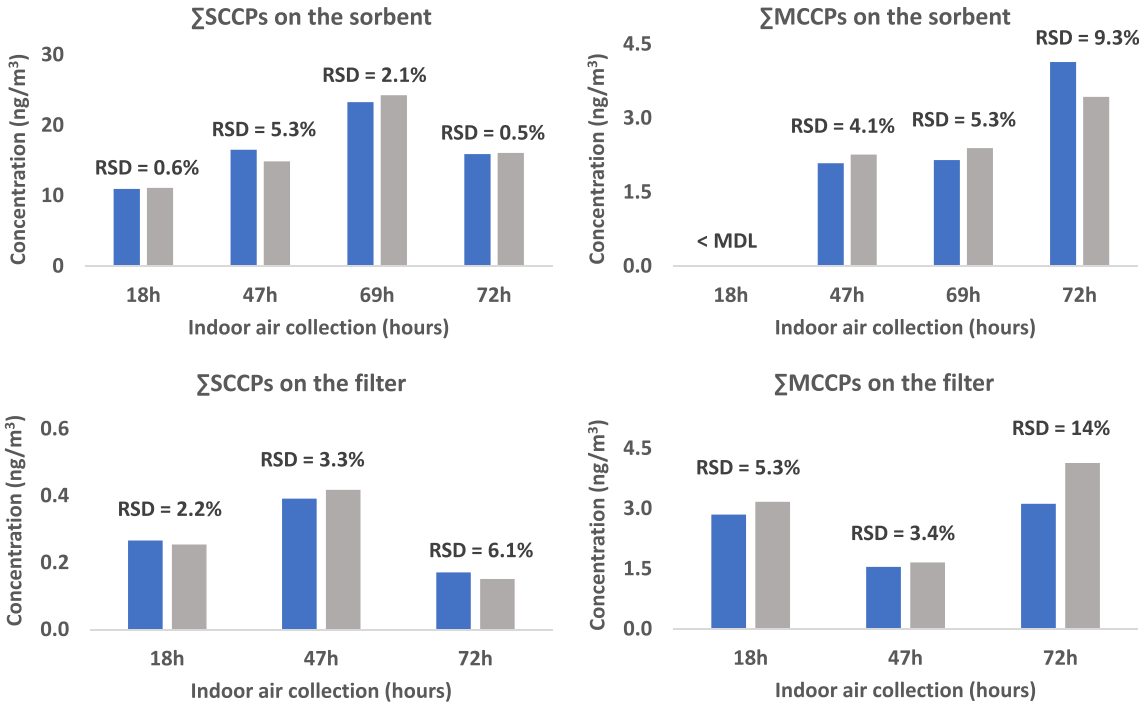

Fig. 2. Indoor air measurement repeatability between parallel samplers on the sorbent (gas phase (A, B)) and filter (particle phase (C, D)) for ΣSCCPs (left) and ΣMCCPs (right), respectively.

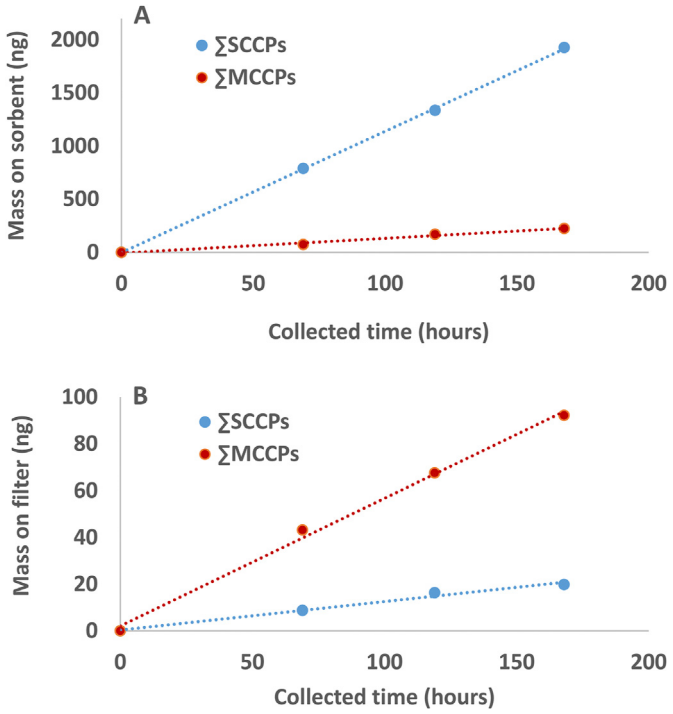

Fig. 3. Mass ΣSCCPs and ΣMCCPs observed on the sorbent (A) and filter (B) after 69, 119- and 168-h air sampling collections to evaluate holding capacity.

(Fig. S4). These results support the breakthrough assessment as we would expect uptake by the sorbent to remain constant (with all other sampling variables remaining constant) until the sorbent capacity has been reached. Linear uptake observed over the entire sampling period shows that accurate measurements can be obtained up to 7 days without loss due to breakthrough. Percentage breakthrough of the filter could not be determined and, therefore, saturation of the filter capacity was assessed. Fig. 3B shows the ΣMCCPs and ΣSCCPs measurements on the particle bound fraction with both a linear trend up to the sampling period of 7 days (168 h). Both profiles show good linearity (R^2 of 0.99 for both the ΣMCCPs and ΣSCCPs), indicating that the filter had not reached its capacity and reliable filter measurements can be obtained after a week of continuous sampling.

This finding was further confirmed by comparison of the CPs patterns on both phases. Generally, the particle bound MCCPs show a different composition to that of the gaseous MCCPs. The gaseous MCCP congener groups show only contribution of the 42% Cl technical formulation, whereas the particle bound MCCP congener groups show a divided pattern between the MCCP 42%, 52% and 57% Cl technical standards. The observed contributions were derived from the Lawson and Hanson algorithm (Bogdal et al., 2015) and are shown in Fig. 4.

The MCCPs on the filter display an average contribution of 43%, 56% and 1% for the MCCP 42%, 52% and 57% Cl technical standards while the gaseous MCCPs show a 100% contribution of the MCCP 42% Cl standard (n = 16). The individual MCCP chain lengths of the gaseous and particle bound fractions were also compared. In both the gas- and particle phase, the C_{14} chain lengths are the most predominant (91% ± 2.1% and 77% ± 2.9%, respectively; n = 16). However, their distributions differ from one to another. The C_{14} chain lengths on the gaseous phase are shifted towards the lower chlorinated congener groups which can be explained by the higher volatility of the lower congener groups, thus, their greater presence within the gas phase. This distribution shift of the C_{14} chain lengths between the gas and particle bound phases was also observed for the breakthrough experiment, as shown in Fig. 5. Contribution and the distribution of the MCCP profiles in both the gas and particle phases show clear differences, indicating that filter breakthrough has not occurred and impacted the sorbent after the 5-day

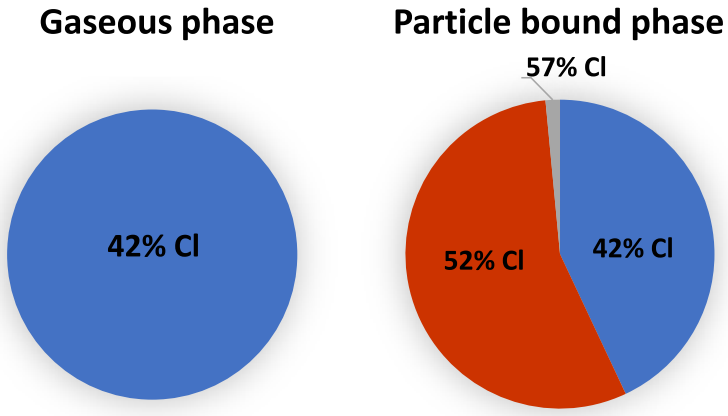

Fig. 4. MCCP contribution of the Dr. Ehrenstorfer GmbH's technical formulations observed on the gaseous and particle bound phase of the samples. Composition of the MCCPs on the sorbent (left) and filter (right). Contributions were obtained from the Lawson and Hanson algorithm (Bogdal et al., 2015) (n = 16).

sampling period. The composition and distribution of the SCCPs was also examined (Figs. S4-5). Previous studies have shown C_{10-11} to be the most abundant in the atmosphere (Section 3.2) due to their high volatility. Within our study, these chain lengths represent 94% and 60% of the ΣSCCP within the gaseous and particle bound phase, respectively. The gas phase consists of 68% (±1.5%) of the C_{10} homologue, whereas the C_{11} homologue is most abundant in the particle bound phase (34% ± 1.3%). As shown in the pie chart (Fig. S6), the composition of the particle bound phase is a divided pattern between all the SCCP chain lengths with the Cl_{7-8} as dominant congener groups. This is not unexpected as a shift towards the higher chlorinated congener groups on the particle bound phase can be explained by their physical-chemical properties and lower vapor pressures.

It is of importance to emphasize that comparison of CP composition can provide essential information, adding more value to statistical evaluation. In addition, distinguishing the CP profiles present in the gas and particle separately is required to determine the accurate concentrations and source elucidation as CPs present in both phases exhibit differences in physical-chemical properties, affecting their environmental fate and decomposition processes. Most CP studies investigating air have combined both phases, losing information regarding sources of exposure to SCCPs and MCCPs or estimation of inhalation intake (gaseous vs particle) which can be crucial for inhalation risk assessment for indoor environments. In addition, the composition of the environmental samples strongly affects quantification as most methodologies depend on the response factor (RF) values. Recent study by Mézière et al. (2020) revealed differences in homologue response patterns between different instrument platforms using quantification methodologies with RF values strongly dependent on %Cl and might require corrections when reporting data. Combination of the gas and particle phases will affect quantification as the CPs of higher chlorination degree on the particle bound phase will increase the RF value, leading to underestimation of the gas phase concentrations. Using the same reasoning, the measurements of the particle bound phase will be overestimated. Thus, the outcomes are often unreliable. Separating the two phases improves comparison with analytical and modelling studies and more importantly, improve data accuracy.

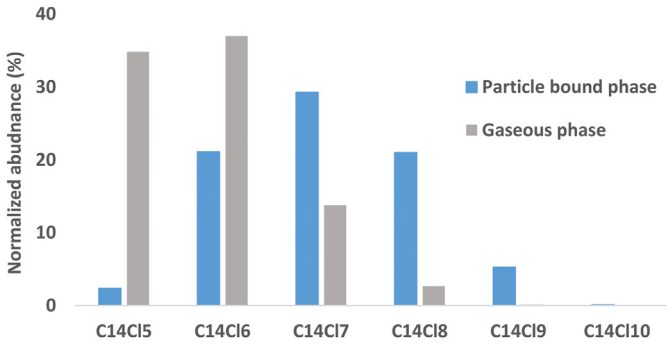

Fig. 5. Distribution of the C_{14} chain lengths observed on the gaseous and particle bound phase for the breakthrough assessment.

3.2. Challenges of CP data comparison

In this study, the indoor gaseous sample concentrations varied from 11 to 24 ng/m^3 (mean of 17 ng/m^3) and 2.1–4.1 ng/m^3 (mean of 2.7 ng/m^3) for the ΣSCCPs and ΣMCCPs, respectively. Indoor concentrations of the particle bound fractions ranged from 0.15 to 0.42 ng/m^3 (mean of 0.28 ng/m^3) and 1.5–4.1 ng/m^3 (mean of 2.7 ng/m^3) for the ΣSCCPs and ΣMCCPs, respectively. Concentration observed outdoors of the Fram Centre building ranged between 0.16 and 0.35 ng/m^3 (mean of 0.27 ng/m^3) for the gaseous ΣSCCPs being one to three orders of magnitude lower compared to indoor measurements. The ΣSCCPs concentration on the sorbent were on average 6-fold greater than the ΣMCCPs concentration (Fig. 2). This is not surprising considering the higher volatility of the SCCPs, therefore prone to partition to the gas phase. Concentration ΣMCCPs on the filter is significantly higher (T-test; one tailed $p < 0.05$) compared to the ΣSCCPs. This is likely due to SCCPs higher vapor pressures and greater presence in the gas phase. Remarkably, the concentration of the MCCPs between the gas and particle phases is equally distributed, even though they were detected in higher abundance on the filters. This phenomenon is caused by the strong dependence of chlorination degree on response factors (RFs) using negative chemical ionization. Steeper slopes were observed for technical formulation with increasing degrees of chlorination (Fig. S2), which have also been observed and explained by several other studies (Li et al., 2017; Reth et al., 2005; Yuan et al., 2017; Zou et al., 2018). MCCP congener groups detected on the sorbent were represented by congeners of lower degree of chlorination (42% Cl), thus lower response slopes. More than 50% of the MCCPs found on the particles was represented by congeners of higher degree of chlorination (52 and 57% Cl, Fig. 4). Thus, concentration levels within the gas phase appear comparable to those observed on the filter (due to the abundance normalized by lower response slope)

even though their overall abundance is much lower. As the composition of the CPs in environmental samples can change spatially and temporally, obtaining accurate and comparable measurements on a ΣSCCPs or ΣMCCPs basis remains a challenge. In addition, comparison of concentrations should be performed with caution as the concentrations also vary depending on the sample- and quantification methodology (van Mourik et al., 2018), the sample type (e.g. gaseous samples, particle bound samples or combined), building space (e.g. office, floor or open indoor spaces) and/or instrumentation ((Krätschmer and Schächtele, 2019); Mézière et al., 2020).

Higher levels of CP within indoor environment found by Gao et al. (2018) and Huang et al. (2017) are not unexpected as China has the largest CP production of any country and thus, a greater emission and exposure to CPs is expected (Glüge et al., 2016). However, the reported concentrations by Gao et al. (2018) (9.77–966 ng/m^3 (mean of 181 ng/m^3) and <0.13–613 ng/m^3 (mean of 41.9 ng/m^3) for the SCCPs and MCCPs, respectively) represent the sum of both gas and particle phase as particles were not filtered during collection, thus gaseous concentrations will be underestimated based on the contribution from the particle bound fraction. This can result in inaccurate concentrations for regulation assessments as it causes a shift in distribution and should be avoided. Interestingly, Huang et al. (2017) detected higher particulate phase (PM_{10}) concentrations of SCCPs (38.3–87.7 ng/m^3 (mean of 61.1 ng/m^3)) compared to MCCPs (3.2–9.6 ng/m^3 (mean of 6.9 ng/m^3)), despite MCCPs being expected to be more dominant in the particle bound phase due to their lower vapor pressures. This could indicate different sources of CPs to particulate matter or greater exposure to SCCPs present in China. Indoor air studies between household buildings resulted in gaseous sample concentrations ranging from <5 to 210 ng/m^3 for ΣS/MCCPs (mean of 69 ng/m^3) (Fridén et al., 2011) and from 1.7 to 54 ng/m^3 (mean of 8.9 ng/m^3) and <0.35–13 ng/m^3 (mean of 1.4 ng/m^3) for the ΣSCCPs and ΣMCCPs, respectively, (Yuan et al., 2021). The wide concentration ranges could be attributed to differences in core materials (e.g., building materials or lubricants) between sampling sites. As the concentrations of the gas and particle bound phase in the study of Fridén et al. (2011) were combined, no evident observation can be drawn concerning the CP contribution to each phase.

Previous outdoor reports in Norway by Borgen et al. (2002) reported higher ΣSCCP concentrations (1.8–10.6 ng/m^3) which is not unexpected as the study was performed prior to the SCCP restriction (Stockholm Convention, 2017) and could be the reflection to greater SCCP usage and sources. However, differences could also be attributed to different analytical and quantification methodologies as mentioned earlier.

Composition of the CPs could also differ between laboratories as shown in interlaboratory comparison studies (Krätschmer and Schächtele (2019)). Studies by van Mourik et al. (2020) and Huang et al. (2017) reported carbon chain lengths of C_{10-11} (SCCPs) and C_{14} (MCCPs) with Cl_{5-6} groups to be the highest in air samples which is in good agreement with the observations within this study. Similar profiles were observed by Ma et al. (2014) with fractions of ΣCl_{5-6}-SCCPs describing 74.7% and 58.4% for the gaseous and particle bound phase, respectively. The C_{14-15}-MCCP fractions were 93.6% (particle bound phase) and 77.2% (gas phase), contrary to our findings (Section 3.2) and expectations as those homologues are considered more volatile. Other studies (Li et al., 2012; Wang et al., 2012) observed shifts among the seasons which could indicate differences in half-lives between the CPs. Hence, more research should be devoted to both quantitative and qualitative analysis of the CPs.

3.3. Detection of vSCCPs within indoor air

Studies on CPs in air with carbon chain lengths <10 is limited or not available at all. Recent study by van Mourik et al. (2020),Xia et al. (2019) and Yuan et al. (2021) detected the very short CPs (vSCCPs) in their air samples during indoor- and outdoor sampling. Within this study, vSCCPs as low as C_5 could easily be detected on the sorbent during indoor air collection. Fig. 6 shows the normalized abundances of the C_5-C_9-CPs and SCCPs extracted from the full spectra with the isotope clusters listed in Table S3. Congener groups < C_{10} were not detected in the field blanks nor in the Dr. Ehrenstorfer and the LGC reference standards. Interestingly, Xia et al. (2019) and Yuan et al. (2021) detected the vSCCPs in their standard mixtures, which warrants further investigation. The shorter chain CPs were particularly abundant on the sorbent, empathizing their high volatility. Some of congener groups of the C_8 and C_9 chain lengths were detected in proportions of equal or greater abundances than congener groups of the C_{11} and C_{12} chain lengths. We assume that those congener groups are produced in processes where mixtures of CPs are used without any restrictions of carbon chain lengths. However, recent findings have shown the formation of vSCCPs through metabolism of CPs via human liver microsomes (He et al., 2020). This indicates that humans will not only undergo exposure to vSCCPs via inhalation (Yuan et al., 2021), but also metabolism, representing a greater exposure risk. As new and more sensitive techniques are available, more attention should be given to these vSCCPs and the need of commercially available standards for quantification. Evaluation regarding their environmental fate (LRTP and degradation) and bioaccumulation and toxicity potential is needed as some of the chain lengths are more

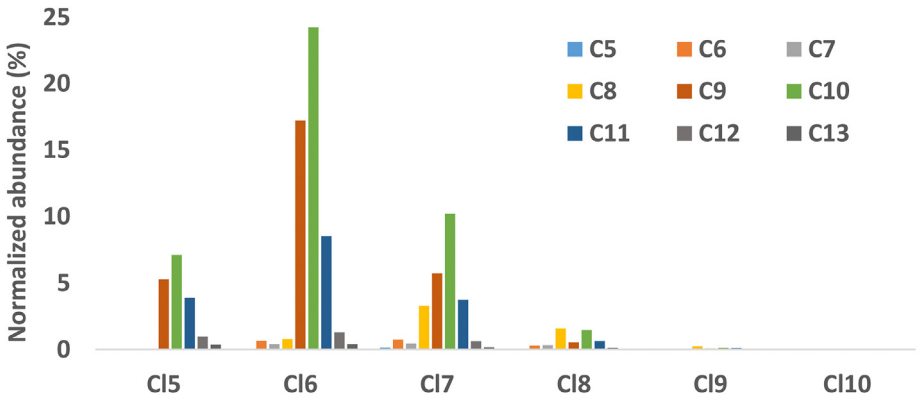

Fig. 6. Congener group abundance profiles of the C_5-C_9 and SCCP detected in an indoor air sampling experiment.

abundant than certain SCCP congener groups.

The developed active air sampler is highly suitable for simultaneous determination of SCCP and MCCP concentrations within indoor gas and particle phase fractions with robust performance after 7 days of continuous sampling. Separation of the gas and particle bound phase reveals differences in congener group profiles and prevents reporting inaccurate concentrations by using response factors reflective of the phase congener profile. Very short chain chlorinated paraffins (vSCCPs: C_5-C_9) within indoor environments were detected in proportions equivalent or greater than some of the SCCP congener groups, which might pose additional inhalation exposure risks or other implications towards human health.

CRediT author statement

Insam Al. Saify: Methodology, Software, Validation, Formal analysis, Investigation, Data curation, Writing – Original Draft, Writing – Review & Editing, Visualization. Lara Cioni: Methodology, Validation, Formal analysis, Investigation. Louise M. van Mourik: Writing – Review & Editing, Supervision. Sicco H. Brandsma: Software, Writing – Review & Editing, Supervision. Nicholas A. Warner: Conceptualization, Methodology, Resources, Writing - original draft, Writing - review & editing, Visualization, Supervision, Project administration, Funding acquisition.

Declaration of competing interest

The authors declare that they have no known competing financial interests or personal relationships that could have appeared to influence the work reported in this paper.

Acknowledgements

Financial support for this study was provided by the Norwegian Ministry of Climate and Environment through the Strategic Institute Programs, granted through the Norwegian Research Council (Arctic, the herald of Chemical Substances of Environmental Concern, Clean Arctic, project #117031) and the Fram Centre Flagship Program “Hazardous substances – effects on ecosystems and human health” (Project 481/762019: Screening for Emerging Arctic health Risks to Circumpolar Human populations (SEARCH)). Financial support was also received through the Erasmus + programme of the European Union. We also thank Svein Knudsen and his team for developing the sampler template (Innovation NILU AS).

Appendix A. Supplementary data

Supplementary data to this article can be found online at https://doi.org/10.1016/j.chemosphere.2021.130066.

Disclaimer

The European Commission’s support for the production of this publication does not constitute an endorsement of the contents, which reflect the views only of the authors, and the Commission cannot be held responsible for any use which may be made of the information contained therein.

References

Bogdal, C., Alsberg, T., Diefenbacher, P.S., Macleod, M., Berger, U., 2015. Fast quantification of chlorinated paraffins in environmental samples by direct injection high-resolution mass spectrometry with pattern deconvolution. Anal. Chem. 87, 2852–2860. https://doi.org/10.1021/ac504444d.

Borgen, A.R., Schlabach, M., Kallenborn, R., Christensen, G., Skotvold, T., 2002. Polychlorinated alkanes in ambient air from Bear Island. Organohalogen Compd. 59, 303–306.

Chen, C., Li, L., Liu, J.J., Liu, J.J., 2019. Global environmental fate of short-chain chlorinated paraffins: modeling with a single vs. multiple sets of physicochemical properties. Sci. Total Environ. 666, 423–430. https://doi.org/10.1016/j.scitotenv.2019.02.157.

Cioni, L., Cincinelli, A., Martellini, T., Warner, N.A., 2018. Development and Evaluation of an Active Air Sampling Method for the Determination of Chlorinated Paraffins. Università degli Studi di Firenze.

Dick, T.A., Gallagher, C.P., Tomy, G.T., 2010. Short- and medium-chain chlorinated paraffins in fish, water and soils from the Iqaluit, Nunavut (Canada), area. World Rev. Sci. Technol. Sustain. Dev. 7, 387–401. https://doi.org/10.1504/WRSTSD.2010.032747.

Fridén, U.E., McLachlan, M.S., Berger, U., 2011. Chlorinated paraffins in indoor air and dust: concentrations, congener patterns, and human exposure. Environ. Int. 37, 1169–1174. https://doi.org/10.1016/j.envint.2011.04.002.

Gao, W., Cao, D., Wang, Yingjun, Wu, J., Wang, Ying, Wang, Yawei, Jiang, G., 2018. External exposure to short- and medium-chain chlorinated paraffins for the general population in beijing, China. Environ. Sci. Technol. 52, 32–39. https://doi.org/10.1021/acs.est.7b04657.

Glüge, J., Schinkel, L., Hungerbühler, K., Cariou, R., Bogdal, C., 2018. Environmental risks of medium-chain chlorinated paraffins (MCCPs): a review. Environ. Sci. Technol. 52, 6743–6760. https://doi.org/10.1021/acs.est.7b06459.

Glüge, J., Wang, Z., Bogdal, C., Scheringer, M., Hungerbühler, K., 2016. Global production, use, and emission volumes of short-chain chlorinated paraffins – a minimum scenario. Sci. Total Environ. 573, 1132–1146. https://doi.org/10.1016/j.scitotenv.2016.08.105.

He, C., van Mourik, L., Tang, S., Thai, P., Wang, X., Brandsma, S.H., Leonards, P.E.G., Thomas, K.V., Mueller, J.F., 2020. In vitro biotransformation and evaluation of potential transformation products of chlorinated paraffins by high resolution accurate mass spectrometry. J. Hazard Mater. https://doi.org/10.1016/j.jhazmat.2020.124245.

Huang, H., Gao, L., Xia, D., Qiao, L., Wang, R., Su, G., Liu, W., Liu, G., Zheng, M., 2017. Characterization of short- and medium-chain chlorinated paraffins in outdoor/indoor PM10/PM2.5/PM1.0 in Beijing, China. Environ. Pollut. 225, 674–680. https://doi.org/10.1016/j.envpol.2017.03.054.

Krätschmer, K., Schächtele, A., 2019. Interlaboratory studies on chlorinated paraffins: evaluation of different methods for food matrices. Chemosphere. https://doi.org/10.1016/j.chemosphere.2019.06.022.

Krätschmer, K., Schächtele, A., Malisch, R., Vetter, W., 2019. Chlorinated paraffins (CPs) in salmon sold in southern Germany: concentrations, homologue patterns and relation to other persistent organic pollutants. Chemosphere 227, 630–637. https://doi.org/10.1016/j.chemosphere.2019.04.016.

Li, Q., Li, J., Wang, Y., Xu, Y., Pan, X., Zhang, G., Luo, C., Kobara, Y., Nam, J.J., Jones, K.C., 2012. Atmospheric short-chain chlorinated paraffins in China, Japan, and South Korea. Environ. Sci. Technol. 46, 11948–11954. https://doi.org/10.1021/es302321n.

Li, T., Wan, Y., Gao, S., Wang, B., Hu, J., 2017. High-throughput determination and characterization of short-, medium-, and long-chain chlorinated paraffins in human blood. Environ. Sci. Technol. 51, 3346–3354. https://doi.org/10.1021/acs.est.6b05149.

Ma, X., Zhang, H., Zhou, H., Na, G., Wang, Z., Chen, C., Chen, Jingwen, Chen, Jiping, 2014. Occurrence and gas/particle partitioning of short- and medium-chain chlorinated paraffins in the atmosphere of Fildes Peninsula of Antarctica. Atmos. Environ. 90, 10–15. https://doi.org/10.1016/j.atmosenv.2014.03.021.

Mézière, M., Cariou, R., Larvor, F., Bichon, E., Guitton, Y., Marchand, P., Dervilly, G., Bruno, L.B., 2020. Optimized characterization of short-, medium, and long-chain chlorinated paraffins in liquid chromatography-high resolution mass spectrometry. J. Chromatogr. A 31, 1885–1895. https://doi.org/10.1016/j.chroma.2020.460927.

Reth, M., Zencak, Z., Oehme, M., 2005. New quantification procedure for the analysis of chlorinated paraffins using electron capture negative ionization mass spectrometry. J. Chromatogr. A 1081, 225–231. https://doi.org/10.1016/j.chroma.2005.05.061.

Sakhi, A.K., Cequier, E., Becher, R., Bølling, A.K., Borgen, A.R., Schlabach, M., Schmidbauer, N., Becher, G., Schwarze, P., Thomsen, C., 2019. Concentrations of selected chemicals in indoor air from Norwegian homes and schools. Sci. Total Environ. 674, 1–8. https://doi.org/10.1016/j.scitotenv.2019.04.086.

Schinkel, L., Bogdal, C., Canonica, E., Cariou, R., Bleiner, D., McNeill, K., Heeb, N.V., 2018. Analysis of medium-chain and long-chain chlorinated paraffins: the urgent need for more specific analytical standards. Environ. Sci. Technol. Lett. 5, 708–717. https://doi.org/10.1021/acs.estlett.8b00537.

UNEP, 2017. n.d. SC-8/11: Listing of Short-Chain Chlorinated Paraffins. United Nations Environmental Programme Stockholm Convention on Persistent Organic Pollutants, Stockholm, Sweden.

Van Mourik, L.M., Leonards, P.E.G., Gaus, C., De Boer, J., 2015. Recent developments in capabilities for analysing chlorinated paraffins in environmental matrices: a review. Chemosphere 136, 259–272. https://doi.org/10.1016/j.chemosphere.2015.05.045.

van Mourik, L.M., van der Veen, I., Crum, S., de Boer, J., 2018. Developments and interlaboratory study of the analysis of short-chain chlorinated paraffins. TrAC Trends Anal. Chem. (Reference Ed.) 102, 32–40. https://doi.org/10.1016/j.trac.2018.01.004.

van Mourik, L.M., Wang, X., Paxman, C., Leonards, P.E.G., Wania, F., de Boer, J., Mueller, J.F., 2020. Spatial variation of short- and medium-chain chlorinated paraffins in ambient air across Australia. Environ. Pollut. 261, 114141. https://doi.org/10.1016/j.envpol.2020.114141.

Wang, T., Han, S., Yuan, B., Zeng, L., Li, Y., Wang, Y., Jiang, G., 2012. Summer-winter concentrations and gas-particle partitioning of short chain chlorinated paraffins in the atmosphere of an urban setting. Environ. Pollut. 171, 38–45. https://doi.org/10.1016/j.envpol.2012.07.025.

Wang, Y., Zhu, X., Gao, Y., Bai, H., Wang, P., Chen, J., Yuan, H., Wang, L., Li, X., Wang, W., 2019. Monitoring gas- and particulate-phase short-chain polychlorinated paraffins in the urban air of Dalian by a self-developed passive sampler. J. Environ. Sci. (China) 80, 287–295. https://doi.org/10.1016/j.jes.2019.01.007.

Warner, N.A., Nikiforov, V., Krogseth, I.S., Bjørnby, S.M., Kierkegaard, A., Bohlin-Nizzetto, P., 2020. Reducing sampling artifacts in active air sampling methodology for remote monitoring and atmospheric fate assessment of cyclic volatile methylsiloxanes. Chemosphere 255, 1–8. https://doi.org/10.1016/j.chemosphere.2020.126967.

Xia, D., Gao, L., Zheng, M., Sun, Y., Qiao, L., Huang, H., Zhang, H., Fu, J., Wu, Y., Li, J., Zhang, L., 2019. Identification and evaluation of chlorinated nonane paraffins in the environment: a persistent organic pollutant candidate for the Stockholm Convention? J. Hazard Mater. 371, 449–455. https://doi.org/10.1016/j.jhazmat.2019.02.089.

Yuan, B., Bogdal, C., Berger, U., MacLeod, M., Gebbink, W.A., Alsberg, T., De Wit, C.A., 2017. Quantifying short-chain chlorinated paraffin congener groups. Environ. Sci. Technol. 51, 10633–10641. https://doi.org/10.1021/acs.est.7b02269.

Yuan, B., Tay, J.H., Padilla-Sánchez, J.A., Papadopoulou, E., Haug, L.S., De Wit, C.A., 2021. Human exposure to chlorinated paraffins via inhalation and dust ingestion in a Norwegian cohort. Environ. Sci. Technol. 55, 1145–1154. https://doi.org/10.1021/acs.est.0c05891.

Zeng, L., Lam, J.C.W., Horii, Y., Li, X., Chen, W., Qiu, J.W., Leung, K.M.Y., Yamazaki, E., Yamashita, N., Lam, P.K.S., 2017. Spatial and temporal trends of short- and medium-chain chlorinated paraffins in sediments off the urbanized coastal zones in China and Japan: a comparison study. Environ. Pollut. 224, 357–367. https://doi.org/10.1016/j.envpol.2017.02.015.

Zhou, W., Shen, M., Lam, J.C.W., Zhu, M., Liu, L., Chen, H., Du, B., Zeng, L., Zeng, E.Y., 2018. Size-dependent distribution and inhalation exposure characteristics of particle-bound chlorinated paraffins in indoor air in Guangzhou, China. Environ. Int. 121, 675–682. https://doi.org/10.1016/j.envint.2018.10.004.

Zou, Y., Niu, S., Dong, L., Hamada, N., Hashi, Y., Yang, W., Xu, P., Arakawa, K., Nagata, J., 2018. Determination of short-chain chlorinated paraffins using comprehensive two-dimensional gas chromatography coupled with low resolution mass spectrometry. J. Chromatogr. A 1581–1582, 135–143. https://doi.org/10.1016/j.chroma.2018.11.004.